Molecular adsorption study of nicotine and caffeine on single-walled carbon nanotubes from first principles

Hyung-June Lee [a], Gunn Kim [b,*], Young-Kyun Kwon [a,*]

[a] Department of Physics and Research Institute for Basic Sciences, Kyung Hee University, Seoul 130-701, Republic of Korea
[b] Department of Physics and Graphene Research Institute, Sejong University, Seoul 143-747, Republic of Korea

ABSTRACT

Using first-principles calculations, we investigate the electronic structures and binding properties of nicotine and caffeine adsorbed on single-walled carbon nanotubes to determine whether CNTs are appropriate for filtering or sensing nicotine and caffeine molecules. We find that caffeine adsorbs more strongly than nicotine. The different binding characteristics are discussed by analyzing the modification of the electronic structure of the molecule-adsorbed CNTs. We also calculate the quantum conductance of the CNTs in the presence of nicotine or caffeine adsorbates and demonstrate that the influence of caffeine is stronger than nicotine on the conductance of the host CNT.

© 2013 Elsevier B.V. All rights reserved.

1. Introduction

Carbon nanotubes (CNTs) have attracted much academic and industrial interest because of their remarkable physical and chemical properties [1–11]. One of the most intriguing characteristics of CNTs is a very large surface area [12–14] comparable to that of activated carbon. This property has been exploited to develop various applications including hydrogen storage, filters removing toxic compounds, and chemical sensors. In spite of the overestimated earlier studies [15–17], however, CNTs did not appear to be a good storage medium for hydrogen due to their inert surfaces, where H_2 molecules adsorb very weakly via van der Waals interaction [18–21]. The binding properties of hazardous molecules on CNTs were also examined theoretically and experimentally [22–26] for potential filter application. One of the most promising applications of CNTs is a sensor application. CNT-based sensors were developed and demonstrated to detect a wide range of molecules such as ammonia [27], nitrogen dioxide [27], oxygen [28], alcohol [29], and other molecules [30–32]. They verified that CNT-based sensors are able to detect not only the type of gas molecule, but also the concentration of the adsorbate.

Nicotine and caffeine are both alkaloids and therapeutic compounds. They serve as stimulants for the central nervous system in humans. Through tobacco and coffee, nicotine and caffeine are addictive drugs used heavily by humans. Because of their psychoactive effects, nicotine and caffeine could have positive effects. For example, nicotine appears to enhance concentration and memory due to the increase of acetylcholine [33], and caffeine seems to

enhance performance in endurance sports [34,35]. However, these drugs often produce side effects. Both of them may increase the heart rate that further limits the ability of the body to maintain homeostasis during exercise. Overdose of these drugs causes severe problems. In particular, nicotine overdose can be deadly, and excessive ingestion of caffeine over extended periods of time results in a toxic condition (caffeinism), with symptoms of vomiting, elevated blood pressure, rapid breathing, heart palpitations, and insomnia. As beverages containing a lot of caffeine to provide mental or physical stimulation, energy drinks have been recently produced. Because they contain more caffeine than strong coffee, some countries have restrictions on the sale and/or manufacture of energy drinks. Therefore, the fabrication of sensors and filters with high sorption capability of these chemicals is desired for public health.

In this letter, we report our study on the adsorption properties of nicotine and caffeine on CNTs. We examined the modification of the electronic structures of CNTs due to adsorbates. We found that both nicotine and caffeine have non-covalent interaction with the CNT through π-stacking. Although both of nicotine and caffeine contain aromatic rings and nitrogen atoms, it was found that they show very different binding geometries and binding energies.

## 2. Computational methods and model structures

We performed first-principles calculations based on density functional theory (DFT) [36,37] to study the structural and electronic properties of the adsorbates on CNTs. We employed a plane-wave basis set and the projector augmented wave (PAW) method implemented in the Vienna ab initio Simulation Package (VASP) [38,39]. The cutoff energy for the kinetic energy was set to 500 eV. The generalized gradient approximation (GGA) [40]

* Corresponding authors. Fax: +82 2 3408 4316.
E-mail addresses: gunnkim@sejong.ac.kr (G. Kim), ykkwon@khu.ac.kr (Y.-K. Kwon).
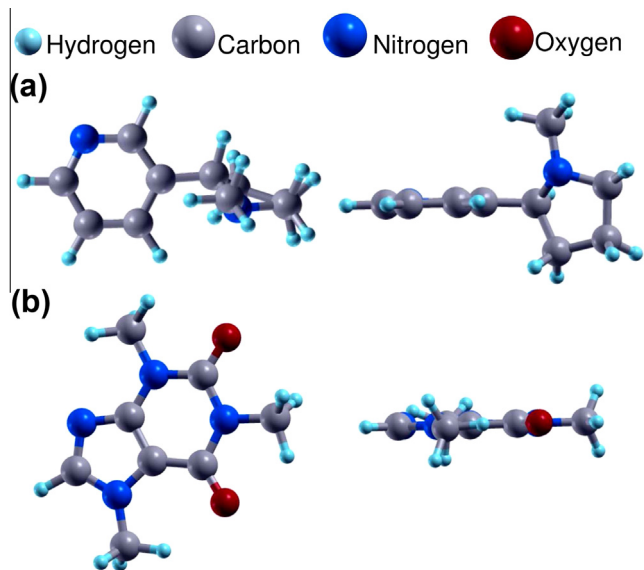
Figure 1. Model structures of (a) nicotine and (b) caffeine. Left: top view. Right: side view.
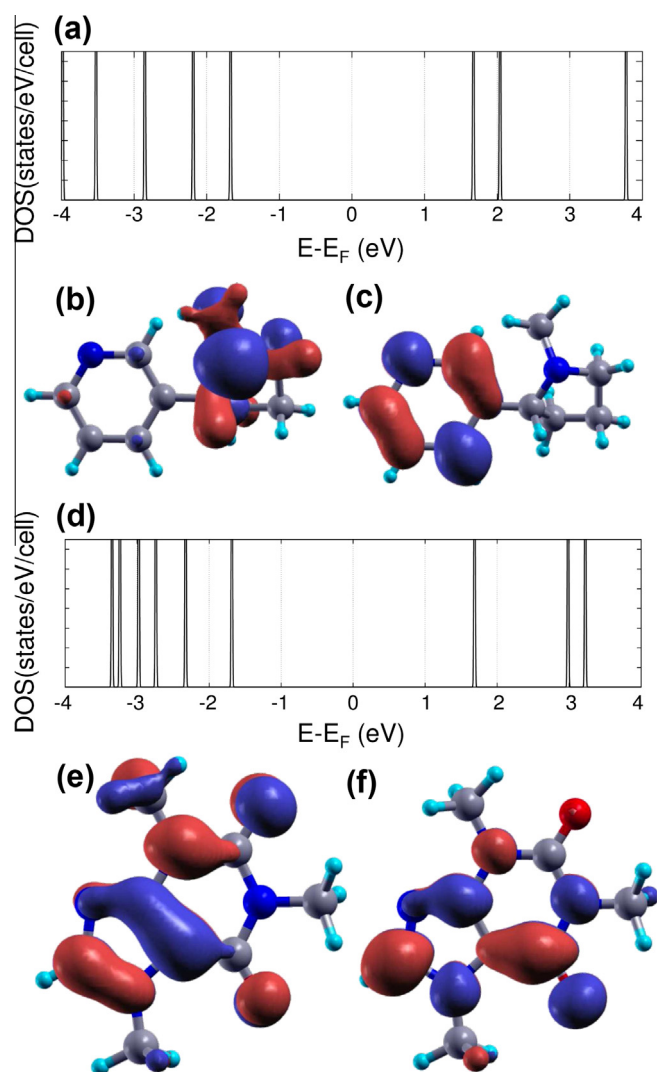

Figure 2. (a) DOS, (b) HOMO and (c) LUMO orbitals of a nicotine molecule. (d) DOS, (e) HOMO and (f) LUMO orbitals of caffeine molecule.

was used to describe the exchange–correlation energy functional. In general, chemical bonding and electron transfer can be described well within the GGA. However, the dispersion or van der Waals (vdW) forces are not represented well by the GGA functional because quantum electronic interactions in the regions of low electron densities are not correctly expressed. In these calculations, thus we made the correction of vdW interaction between the adsorbates and the CNT, using Grimme's method[41] for the GGA (i.e., the GGA plus vdW).

To verify the validity of our computational results, we also repeated our work with the linear combination of pseudoatomic orbitals implemented in the SIESTA code [42,43]. We used 210 Ry as the mesh cutoff energy and double-ζ basis with polarization for the basis set. All the model structures were relaxed until none of the residual forces acting on any atom would exceed 0.03 eV/a_B, where a_B is the Bohr radius. The binding energies were corrected using the basis set superposition error correction with ghost atoms.

The binding energies, electronic band structures, and wavefunctions presented in this letter were all obtained using the pseudoatomic orbital basis set implemented in the SIESTA package. The general trends in the binding energies and the electronic structures for nicotine and caffeine are very similar for the two computational packages (the VASP and SIESTA codes).

We selected the semiconducting (8, 0) CNT as the host material for molecular adsorption. We used a tetragonal supercell with a length of 16.94 Å along the CNT axis and 20 Å along the lateral directions. We utilized $1 \times 1 \times 4$ Monkhorst–Pack sampling [44] for the Brillouin zone integrations. On the other hand, a cubic supercell with a length of 20 Å along all three directions and only one k point at the Γ point were used for calculations of the isolated molecules (nicotine and caffeine). Charge transfer between the adsorbate and the host CNT was estimated using the Bader charge analysis. For each configuration, we obtained its binding energy (E_b) defined by
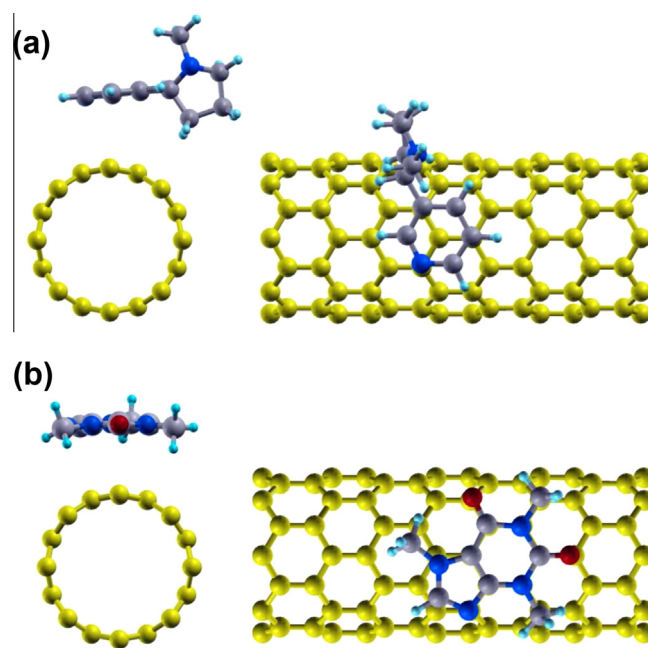

Figure 3. Optimized structure of the (8, 0) CNT with (a) an adsorbed nicotine molecule and (b) an adsorbed caffeine molecule. The figures on the left hand side show side view, whereas the right hand side figures do top view. To avoid confusion, the carbon atoms in the CNT are shown in yellow. (For interpretation of the references to colour in this figure legend, the reader is referred to the web version of this article.)

$$E_{b} = E[CNT] + E[molecule] - E[CNT + molecule],$$

where $E[CNT + molecule]$ and $E[CNT]$ are the total energies of the CNT with and without a nicotine (or caffeine) molecule, respectively, and $E[molecule]$ represents the energy of an isolated nicotine (or caffeine) molecule.

The quantum transport calculations were performed using the TranSIESTA code, based on DFT, and the self-consistent electronic structure of a nanostructure connected to the electrodes. Non-equilibrium Green's functions were used to solve an open system from the DFT Hamiltonian. In the calculations of the quantum transport, $1 \times 1 \times 36k$ points were used in the Monkhorst–Pack scheme [44].
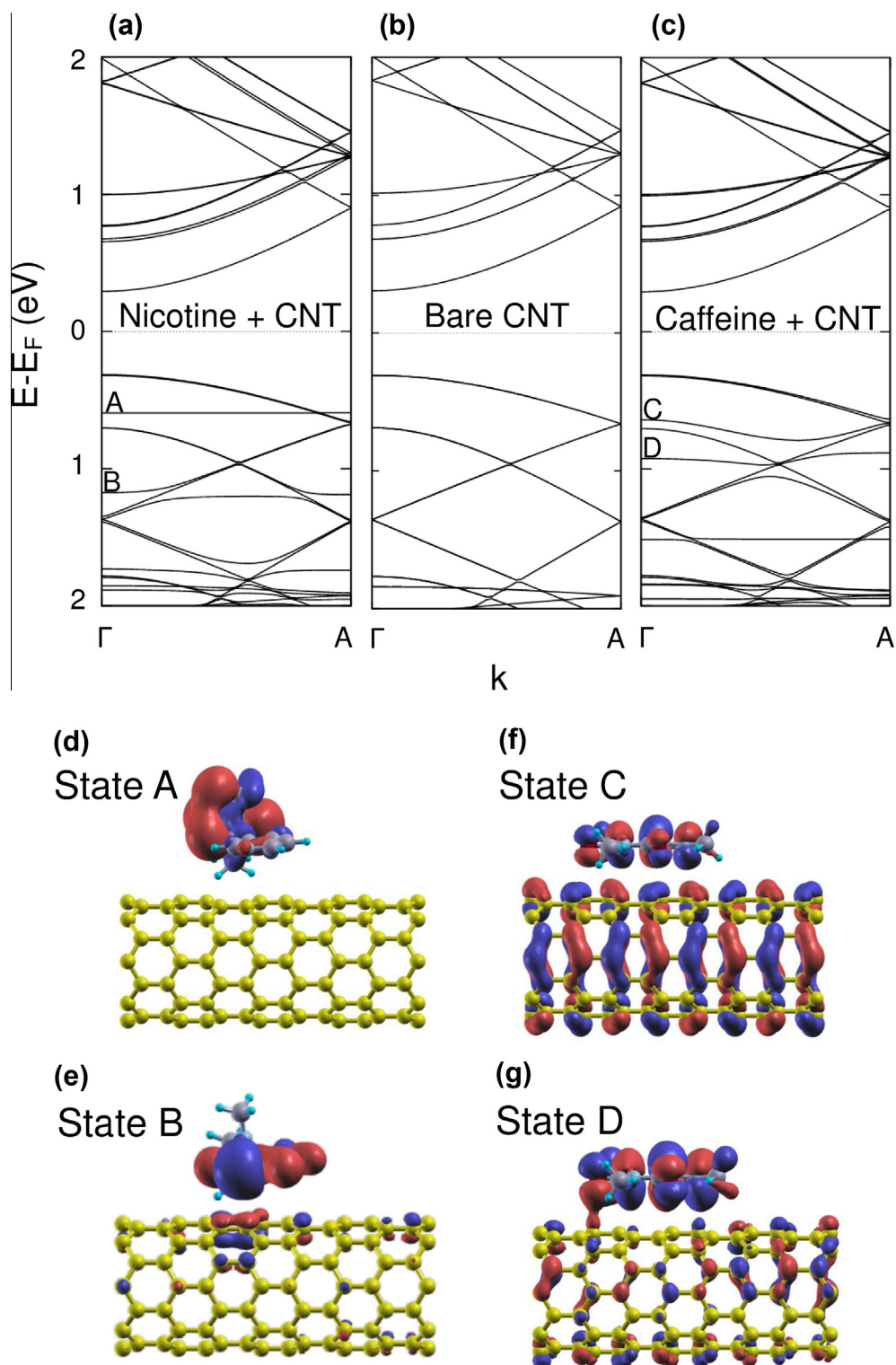
Figure 4. Band structures of (a) the nicotine-adsorbed CNT, (b) the bare (8, 0) CNT and (c) the caffeine-adsorbed CNT. (d and e) The states A and B indicate wavefunctions at labeled "A" and "B" in (a). (f and g) The states C and D indicate wavefunctions at labeled "C" and "D" in (c). The red and blue surfaces indicate the phase of the wave functions. (For interpretation of the references to colour in this figure legend, the reader is referred to the web version of this article.)

3. Results and discussion

First, we calculated the individual nicotine and caffeine molecules in the vacuum condition to optimize the gas phase geometry. Figure 1a and b show the optimized geometries of nicotine and caffeine molecules. All the nitrogen atoms form essentially a planar structure with carbon atoms implying sp^2 orbital hybridization, maintaining the aromatic characteristics.

Figure 2a–c show the density of states (DOS), the highest occupied molecular orbital (HOMO) and the lowest unoccupied molecular orbital (LUMO) of a nicotine molecule, respectively. Similarly, Figure 2d–f represent the same quantities of a caffeine molecule. The energy gaps between the HOMO and the LUMO levels are 3.34 eV and 3.37 eV for the nicotine and caffeine molecules, respectively, which are very similar to each other. However, the energy difference between the LUMO and LUMO+1 (the state one level above the LUMO) of the nicotine molecule in Figure 2a is much smaller that of the caffeine molecule in Figure 2d. Interestingly, the HOMO of nicotine is dominant at the five-membered ring as shown in Figure 2b, whereas the electronic density in the LUMO is high at the phenyl group (six-membered ring) as displayed in Figure 2c. In contrast, the HOMO and LUMO wavefunctions of caffeine appear to be distributed over the whole molecule as shown in Figure 2e and f.

Figure 3 shows the optimized structures of the (8, 0) CNTs with adsorbed nicotine and caffeine molecules. As shown in Figure 3a, the nicotine molecule prefers to contact with the CNT through its six-membered ring rather than its five-membered ring. Moreover, the most stable binding geometry appears similar to Bernal ("AB") stacking of graphite with the binding energy of $E_b \approx 0.46$ eV and the binding distance of $d_b \approx 3.29$ Å. On the other hand, the caffeine molecule is bound to the CNT stronger than the nicotine molecule (almost twice). Its binding energy and distance are $E_b \approx 0.88$ eV and $d_b \approx 3.25$ Å, respectively. It is noteworthy that according to an *ab initio* study of Debbichi et al., the binding energy of antracene on the (10, 10) CNT is ~1 eV when the van der Waals interaction is considered [45]. Our charge analysis demonstrates that no appreciable charge transfer occurs between the molecules and the CNT. Then, what makes the difference in the binding energy for the two types of molecules? Unlike nicotine, a hexagon and a pentagon in caffeine are both on the same plane, and thus this planar

structure enhances the π stacking with the CNT surface. In contrast to AB stacking in the nicotine adsorption, the caffeine molecule prefers "AA" to AB stacking, which is only ~5 meV less stable though.

Figure 4 displays the electronic structures of the bare, nicotine-, and caffeine-adsorbed (8, 0) CNTs. The bare (8, 0) CNT has an energy band gap of 0.58 eV (Figure 4b), whereas both nicotine- and caffeine-adsorbed CNTs increase their band gap to ~0.61 eV, as seen in Figure 4a and c. In Figure 4a–c, we did not find a significant shift in the Fermi level by the molecular adsorption implying no significant charge transfer between the adsorbate and the CNT. In each of the band structure of the molecule-adsorbed CNT, there are two flat bands originating from the molecule. For nicotine (caffeine), such flat bands are located near 0.6 eV (0.6 eV) and 1.3 eV (0.9 eV) below the Fermi level. Figure 4d and e display the wavefunctions corresponding to the states labeled "A" and "B" in Figure 4a at the Γ point. The state A in Figure 4d shows a localized state corresponding to the HOMO of nicotine, whereas the state B exhibits a weakly hybridized π state on the CNT together with the nicotine HOMO−1 state (the state just below the HOMO). As shown in Figure 2b, the electronic density in the HOMO of nicotine is mainly at the five-membered ring and thus it has no practical coupling with any CNT state. Similarly, we show in Figure 4f and g the wavefunctions at the Γ point for the two states labeled "C" and "D" for the caffeine adsorption in Figure 4c. Interestingly, due to the stronger interaction of caffeine with the CNT than that of nicotine via π-stacking, the state C corresponding to the HOMO state of caffeine shows interaction between an extended state of the CNT and a molecular orbital of caffeine.

In 2010, Girão et al. investigated nicotine adsorption on the single-walled CNT [46]. Thus, we need to compare the differences between their models and ours. For the binding energy, our model has stronger adsorption than their models for nicotine adsorbed on the CNT. For the band structure, their models have localized states originating from the nicotine molecule in the forbidden band (just above the valence band top). In contrast, our most stable model for nicotine-adsorbed CNT has no localized state in the forbidden band (see Figure 4).

For further analysis, we calculated charge density differences shown in Figure 5. Isodensity surfaces indicate the regions of electron accumulation (red) and depletion (blue). It is shown that the
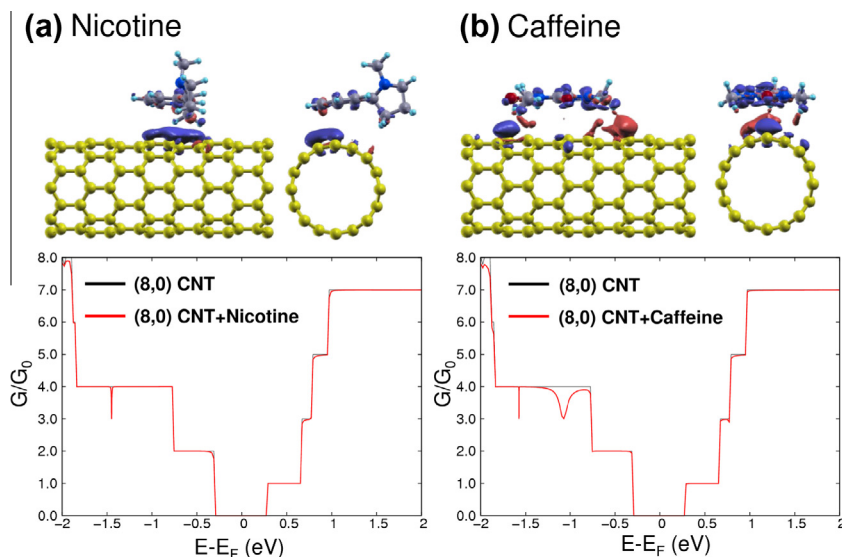
Figure 5. Charge density difference and quantum conductance plots of (a) nicotine- and (b) caffeine-adsorbed CNTs. In the charge density difference plots, red and blue colors represent regions of electron accumulation and depletion, respectively. Here, G_0 (= $2e^2/h$) represents the conductance quantum, where e is called the elementary charge ($\approx 1.602 \times 10^{-19}$ C) and h is the Planck constant ($\approx 1.436 \times 10^{-15}$ eV s). (For interpretation of the references to colour in this figure legend, the reader is referred to the web version of this article.)

nicotine molecule creates a local polarized region at the CNT near the adsorbate as shown in Figure 5b. We found a more interesting feature in the caffeine-adsorbed CNT, where an electron depletion takes place near the O atom bonded to the C atom between two N atoms in the six-membered ring of the caffeine molecule. At the same time, an electron accumulation occurs at the opposite end of the adsorbate (near the five-membered ring). This phenomenon can be interpreted as a "donation and back-donation" between the CNT and the caffeine molecule in the axial direction of the CNT. It is noteworthy that the DFT calculation does not describe accurately the amount of charge transfer but it guarantees the overall shape of isodensity surfaces.

Finally, we present the quantum conductance plots of the (8, 0) CNTs with the adsorbed nicotine and caffeine molecules. As shown in Figure 5, only caffeine gives rise to a broad conductance dip about 1.1 eV below the Fermi level with the reduction of conductance from $4G_0$ to $3G_0$, which is attributed to the state C in Figure 4f. Here, G_0 (= $2e^2/h$) represents the conductance quantum, where e is called the elementary charge ($\approx 1.602 \times 10^{-19}$ C) and h is the Planck constant ($\approx 1.436 \times 10^{-15}$ eV s). On the other hand, both of nicotine and caffeine molecules give rise to very narrow dips in conductance (from $4G_0$ to $3G_0$) around 1.5 eV below the Fermi level, which are related to the states B and D in Figure 4e and g, respectively. As mentioned above, the state C corresponds to the HOMO of caffeine strongly coupled to the extended CNT state, whereas the states B and D originate from the HOMO−1 states of nicotine and caffeine and they are very weakly hybridized with CNT states, respectively. We note that the energy levels of conductance dips may have an offset with those of energy eigenstates. The wavefunctions and the electronic band structures are obtained for a finite CNT with an adsorbed molecule in periodic boundary conditions. In contrast, the quantum conductance is calculated for a finite CNT with an adsorbate molecule connected to two semi-infinite perfect CNTs (electrodes) in both sides. Therefore, the energy offset may occur between the quantum electron conductance and energy eigenstates. Consequently, the caffeine molecule using a CNT-based device can be monitored in the current–voltage (I–V) measurement. In the case of nicotine, on the other hand, it is difficult to detect the molecule using a CNT-based electronic device. Therefore, one should use the CNTs to filter nicotine molecules.

4. Conclusion

In conclusion, we have investigated the electronic and binding properties of nicotine and caffeine molecules on (8, 0) single-walled carbon nanotubes using first-principles calculations. We found that both adsorbates show different binding characteristics on CNTs. The nicotine molecule binds to the CNT with an adsorption energy of 0.46 eV, whereas the caffeine molecule adsorbs with a higher binding energy of 0.88 eV. To figure out the difference, we discussed the modification of the electronic structures of the nicotine- and caffeine-adsorbed CNTs. Although there is no significant charge transfer between the CNT and the adsorbate, we found that there is an noticeable interaction between them. In particular, the caffeine-adsorbed CNT exhibits a special binding feature formed by electron donation and back-donation. Our study of quantum transport demonstrates that I–V curves can distinguish nicotine from caffeine using a CNT-based electronic sensor. We believe our findings of the adsorption properties of caffeine and nicotine on the CNT will help the future studies of intermolecular interaction between the host nanotube and other organic molecules.

References

[1] L. Chico, V.H. Crespi, L.X. Benedict, S.G. Louie, M.L. Cohen, Phys. Rev. Lett. 76 (1996) 971.
[2] S.J. Tan, A.R.M. Verschueren, C. Dekker, Nature 393 (1998) 49.
[3] Y.-K. Kwon, D. Tománek, S. Iijima, Phys. Rev. Lett. 82 (1999) 1470.
[4] Z. Yao, H.W.Ch. Postma, L. Balents, C. Dekker, Nature 402 (1999) 273.
[5] S. Sanvito, Y.-K. Kwon, D. Tománek, C.J. Lambert, Phys. Rev. Lett. 84 (2000) 1974.
[6] S. Berber, Y.-K. Kwon, D. Tománek, Phys. Rev. Lett. 84 (2000) 4613.
[7] C. Zhou, J. Kong, E. Yenilmez, H. Dai, Science 290 (2000) 1552.
[8] J. Lee et al., Nature 415 (2002) 1005.
[9] G. Kim, S.B. Lee, T.-S. Kim, J. Ihm, Phys. Rev. B 71 (2005) 205415.
[10] J.-C. Charlier, X. Blase, S. Roche, Rev. Mod. Phys. 79 (2007) 677.
[11] W.I. Choi, J. Ihm, G. Kim, Appl. Phys. Lett. 92 (2008) 193110.
[12] R.Q. Long, R.T. Yang, Ind. Eng. Chem. Res. 40 (2001) 4288.
[13] M. Cinke, J. Li, B. Cen, A. Cassell, L. Delzeit, J. Han, M. Meyyappan, Chem. Phys. Lett. 365 (2002) 69.
[14] Y.F. Yin, T. Mays, B. McEnanaey, Langmuir 15 (1999) 871.
[15] A.C. Dillon, K.M. Jones, T.A. Bekkedahl, C.H. Kiang, D.S. Bethune, M.J. Heben, Nature 386 (1997) 377.
[16] A. Chambers, C. Park, R.T.K. Baker, N.M. Rodriguez, J. Phys. Chem. B 102 (1998) 4253.
[17] P. Chen, X. Wu, J. Lin, K.L. Tan, Science 285 (1999) 91.
[18] C. Liu, Y.Y. Fan, M. Liu, H.T. Cong, H.M. Cheng, M.S. Dresselhaus, Science 286 (1999) 1127.
[19] C.C. Ahn, Y. Ye, B.V. Ratnakumar, C. Witham, R.C. Bowman Jr., B. Fultz, Appl. Phys. Lett. 73 (1998) 3378.
[20] B. Panella, M. Hirscher, S. Roth, Carbon 43 (2005) 2209.
[21] Y.-K. Kwon, J. Korean Phys. Soc. 57 (2010) 778.
[22] R.Q. Long, R.T. Yang, J. Am. Chem. Soc. 123 (2001) 2058.
[23] X.J. Peng, Y.H. Li, Z.K. Luan, Z.C. Di, Y.H. Wang, B.H. Tian, Z.P. Jia, Chem. Phys. Lett. 376 (2003) 154.
[24] S.B. Fagan et al., Nano Lett. 4 (2004) 1285.
[25] S.B. Fagan, E.C. Girão, J. Mendes, A.G. Souza, Int. J. Quantum Chem. 106 (2006) 2558.
[26] F. Tournus, S. Latil, M.I. Heggie, J.C. Charlier, Phys. Rev. B 72 (2005) 075431.
[27] J. Kong, N. Franklin, C. Zhou, M. Chapline, S. Peng, K. Cho, H. Dai, Science 287 (2000) 622.
[28] P.G. Collins, K. Bradley, M. Ishigami, A. Zettl, Science 287 (2000) 1801.
[29] H.J. Song et al., J. Phys. Chem. C 112 (2008) 629.
[30] K. Bradley, J.-C.P. Gabriel, A. Star, G. Gruener, Appl. Phys. Lett. 83 (2003) 3821.
[31] M.-F. Yu, B.S. Files, S. Arepalli, R.S. Ruoff, Phys. Rev. Lett. 84 (2000) 5552.
[32] P. Burt, N.R. Wilson, J.M.R. Weaver, P.S. Dobson, J.V. Macpherson, Nano Lett. 5 (2005) 639.
[33] J. Rusted, L. Graupner, N. O'Connell, C. Nicholls, Psychopharmacology 115 (1994) 547.
[34] D. Bishop, Sports Med. 40 (2010) 995.
[35] S.A. Conger, G.L. Warren, M.A. Hardy, M.L. Millard-Stafford, Int. J. Sport Nutr. Exercise Metab. 21 (2011) 71.
[36] P. Hohenberg, W. Kohn, Phys. Rev. 136 (1964) B864.
[37] W. Kohn, L.J. Sham, Phys. Rev. 140 (1965) A1133.
[38] G. Kresse, J. Hafner, J. Phys. Rev. B 47 (1993) R558.
[39] G. Kresse, J. Furthmüller, Phys. Rev. B 54 (1996) 11169.
[40] J.P. Perdew, K. Burke, M. Ernzerhof, Phys. Rev. Lett. 77 (1996) 3865.
[41] S. Grimme, J. Comput. Chem. 27 (2006) 1787.
[42] D. Sánchez-Portal, P. Ordejón, E. Artacho, J.M. Soler, Int. J. Quantum Chem. 65 (1997) 453.
[43] E. Artacho, D. Sánchez-Portal, P. Ordejón, A. García, J.M. Soler, Phys. Status Solidi B 215i (1999) 809.
[44] H.J. Monkhorst, J.D. Pack, Phys. Rev. B 13 (1976) 5188.
[45] L. Debbichi, Y.J. Dappe, M. Alouani, Phys. Rev. B 85 (2012) 045437.
[46] E.C. Girão, S.B. Fagan, I. Zanella, A.G. Souza Filho, J. Hazard. Mater. 184 (2010) 678.